

RESEARCH

Open Access



Intelligent electrical equipment fiber Bragg grating temperature measurement system

Anhua Peng^{1,2}, Chengwen Liu^{1,2*} and Le Yang^{1,2}

*Correspondence:
1993000009@jou.edu.cn
¹ School of Mechanical
Engineering, Jiangsu
Ocean University,
Lianyungang 222005,
Jiangsu, China
Full list of author information
is available at the end of the
article

Abstract

Fiber Bragg gratings are widely used in electrical equipment monitoring, structural health monitoring, power system fault monitoring and other actual detection occasions due to the unique advantages of anti-electromagnetic interference, low fusion loss, high sensitivity, small size, and easy distributed measurement. Fiber grating has been widely used in actual detection occasions such as electrical equipment monitoring, structural health monitoring, and power system fault monitoring. The temperature measurement of the motor based on fiber grating sensing technology not only has strong anti-electromagnetic interference ability, but also can realize multi-point distributed temperature measurement. The research on fiber grating temperature measurement system for intelligent electrical equipment is of great significance. This article mainly studies the optical fiber grating temperature measurement system of intelligent electrical equipment. This paper designs the temperature measurement system architecture, including data acquisition layer, data monitoring layer and remote monitoring layer. Complete the system design from two aspects: hardware design and software design. In the hardware part, the functions of the temperature sensor module transmission system, signal demodulation system, PLC and host computer are analyzed. Use FTM3501 fiber temperature converter is used to realize the automatic electrical fiber grating. Experimental results show that the thermometer has alarm and display analysis functions. The measurement uncertainty is analyzed, and the uncertainty of the calibration result of the fiber Bragg grating temperature sensor is 0.0725 °C; the fault judgment time of the system in this paper does not exceed 4.73 s, while the fault judgment time of the control group is more than 4.73 s. Compared with the control group, it has a faster fault accuracy speed. The system has high measurement accuracy and good stability, can be applied to actual temperature measurement systems, and has certain practical value.

Keywords: Fiber Bragg grating, Temperature sensor, Automatic temperature measurement, Electrical equipment

1 Introduction

Nowadays, with the rapid development of society and the continuous progress of science and technology, the industry subdivision is constantly strengthened, and the external conditions required for work in each industry are becoming more and more stringent. Only when sufficient conditions are met can the normal work of each part

of the system be guaranteed and the equipment can operate in a coordinated manner. These conditions are precisely the fact that the industries of various industries are continuously subdivided and can operate normally. A complete set of equipment contains many modules. To ensure the normal operation of the equipment, each part of the system is required to work in a stable environment to meet the actual needs. As the equipment continues to develop in the direction of miniaturization and intelligence, the monitoring sensors must be very small and can form a network to measure the entire system. Optical fiber distribution sensing technology is a detection technology that uses the one-dimensional spatial characteristics of optical fibers to detect multiple signals in different spaces. This technology can measure the change of temperature and strain information in the field with time, so it can be used in many fields.

Temperature is a physical quantity that characterizes how hot or cold an object is. The first parameter that needs to be accurately measured for monitoring special equipment is temperature. On the one hand, because temperature is the main parameter that needs to be constantly measured and controlled in electrical equipment and scientific experiments; on the other hand, because changes in temperature may cause changes in strain and changes in concentration and pressure, real-time temperature monitoring is carried out by electrical. The premise and fundamental of the normal operation of the equipment. The temperature sensing system composed of multiple fiber gratings uses a single optical cable to achieve quasi-distributed measurement. Due to a series of excellent characteristics of fiber grating sensors, choosing fiber grating sensors for experiments and applying it to the health monitoring of electrical equipment will have a huge impact.

The temperature of electrical equipment during operation restricts the safety of high-voltage or extra-high voltage distribution systems. Singh proposed a fiber Bragg grating (FBG) sensor, which can be surface mounted for simultaneous strain and temperature measurement. By embedding conventional FBG sensors in composite laminates, local birefringence is introduced, which causes the bandwidth of the FBG spectrum to vary with strain and temperature. In this way, temperature and strain can be determined simultaneously from two FBG spectral parameters, namely spectral bandwidth and Bragg wavelength. He discussed techniques for improving the spectrum of FBG composite sensors and determining strain and temperature inversely from the measured FBG spectral parameters. The FBG composite sensor has been tested mechanically to verify the performance of the sensor [1]. His method takes too long to judge the fault and cannot achieve the effect of practical application. Zhang proposed an improved Φ -OTDR system based on ultra-weak fiber Bragg grating array to use narrow pulses to achieve quantitative strain measurement, which can extend the detectable fiber length [2]. His method is more complicated and inefficient. Gan proposed a new framework that uses fiber Bragg grating (FBG) sensors to quantify the probability of crack size. Compared with XFEM, standard FEM can more accurately represent the area near the singular point of the crack tip; however, as the size of the crack changes, it needs to be joined again. In addition to the classic four-term asymptotic enrichment function in XFEM, he proposed the integration of higher-order functions to further improve the accuracy of the stress field under the reflection intensity spectrum.

Derive the wavelength of the reflection intensity spectrum as tomographic sensitivity, use five parameters to create a basic model, and quantify the relationship with the crack size [3, 4].

In this paper, on the basis of the principle of fiber grating temperature sensing and the feasibility analysis of the application of intelligent electrical equipment temperature detection. Optical fiber sensor can realize the precise measurement of electromagnetic, mechanical, temperature, chemical composition and other physical quantities. Compared with traditional sensors, it has the advantages of high sensitivity, fast response, anti-electromagnetic interference, corrosion resistance, and electrical insulation. This topic designs and implements an intelligent electrical equipment fiber grating temperature measurement system, which uses the temperature sensitivity of fiber grating in real time Monitor the temperature of electrical equipment, and when the temperature of the monitoring point exceeds the set alarm limit, send out an alarm signal in time to achieve the purpose of finding hidden faults in advance, prompting the operator to deal with the fault in time, and improving the safety and reliability of electrical equipment.

2 Fiber grating sensing model

2.1 Strain sensing model

Of all the external factors that cause the Bragg wavelength drift of the grating, the most direct is the strain parameter, because whether the grating is stretched or compressed, it will inevitably lead to the change of the grating period Λ , and the optical fiber itself has an elastic-optic effect that makes effective refractive index rate n_{eff} also changes with the change of the external stress state. This makes the fiber grating sensor better sense temperature changes. This provides the most basic physical characteristics for the fiber strain sensor made of fiber Bragg grating [4]. Stress-induced Bragg wavelength drift of the grating can be described by Eq. (1).

Where $\Delta\Lambda$ represents the elastic deformation of the fiber itself under the action of stress, Δn_{eff} represents the elastic-optical effect of the fiber, and different stress conditions in the outside world will cause Δn_{eff} different changes from $\Delta\Lambda$. In general, for fiber grating, because it belongs to an isotropic cylindrical structure, the stress applied to it can always be decomposed into three directions of σ_r , σ_θ and σ_z in the cylindrical coordinate system [5, 6]. Only the strain sensing model of pure axial stress is discussed here. According to the characteristics of the cylindrical coordinate system and the main research objective of this article, this article only discusses the strain sensing model of pure axial stress. The advantage of pure axial stress is that the force is stable and not easy to deform.

(1) The general form of Hooke's theorem can be expressed by the following formula:

$$\sigma_i = C_{ij} \cdot \varepsilon_j \quad (i, j = 1, 2, 3, 4, 5, 6) \quad (1)$$

where σ_i is the stress tensor, C_{ij} is the elastic modulus, and ε_j is the strain tensor. For isotropic media, due to the symmetry of the material, C_{ij} can be simplified, and the lame constant λ , μ is obtained:

$$\begin{bmatrix} \sigma_1 \\ \sigma_2 \\ \sigma_3 \\ \sigma_4 \\ \sigma_5 \\ \sigma_6 \end{bmatrix} = \begin{bmatrix} \lambda + 2\mu & \lambda & \lambda & 0 & 0 & 0 \\ \lambda & \lambda + 2\mu & \lambda & 0 & 0 & 0 \\ \lambda & \lambda & \lambda + 2\mu & 0 & 0 & 0 \\ 0 & 0 & 0 & \mu & 0 & 0 \\ 0 & 0 & 0 & 0 & \mu & 0 \\ 0 & 0 & 0 & 0 & 0 & \mu \end{bmatrix} \cdot \begin{bmatrix} \varepsilon_1 \\ \varepsilon_2 \\ \varepsilon_3 \\ \varepsilon_4 \\ \varepsilon_5 \\ \varepsilon_6 \end{bmatrix} \tag{2}$$

where lame constant λ , μ is expressed by the material elastic modulus E and Poisson's ratio ν as:

$$\begin{cases} \lambda = \frac{\nu \cdot E}{(1 + \nu)(1 - 2\nu)} \\ \mu = \frac{E}{2(1 + \nu)} \end{cases} \tag{3}$$

This formula is the general form of Hooke's theorem in homogeneous media. For the optical fiber, because it is a rotating system, it usually uses stress and strain representation at rotational coordinates, that is, the subscript in the above formula is changed to a combination of (r, φ, z) to represent the longitudinal, transverse and shear strains [7].

(2) Fiber grating sensing model under the action of uniform axial stress

Uniform axial stress refers to the longitudinal stretching or compression of the fiber grating. At this time, the stress in each direction can be expressed as $\sigma_{zz} = -P$ (P is the external pressure), $\sigma_{rr} = \sigma_{\theta\theta} = 0$, and there is no tangential stress [8]. According to formula (2), strain in each direction can be obtained as in formula (4). Where E and ν are the elastic modulus and Poisson's ratio of the quartz optical fiber, respectively. Now the strain values in all directions under the effect of uniform axial stress have been obtained, and the stress sensitivity coefficient of fiber gratings is further solved based on this.

$$\begin{pmatrix} \varepsilon_{rr} \\ \varepsilon_{\theta\theta} \\ \varepsilon_{zz} \end{pmatrix} = \begin{pmatrix} \frac{\nu P}{E} \\ \frac{\nu P}{E} \\ -\frac{P}{E} \end{pmatrix} \tag{4}$$

Expand formula (1) to:

$$\Delta n_{eff} = 2\Lambda \left(\frac{\partial n_{eff}}{\partial L} \cdot \Delta L + \frac{\partial n_{eff}}{\partial a} \cdot \Delta a \right) + 2 \frac{\partial \Lambda}{\partial L} \cdot \Delta L \cdot n_{eff} \tag{5}$$

Among them, ΔL is the longitudinal expansion and contraction of the optical fiber, $\partial n_{eff} / \partial L$ is the elastic-optical effect, and $\partial n_{eff} / \partial a$ is the waveguide effect. The relative dielectric impermeability tensor β_{ij} has the following relationship with the dielectric constant ε_{ij} :

$$\beta_{ij} = 1/\varepsilon_{ij} = 1/n_{ij}^2 \tag{6}$$

$$\Delta(\beta_{ij}) = \Delta\left(\frac{1}{n_{ij}^2}\right) = -\frac{2\Delta n_{\text{eff}}}{n_{\text{eff}}^3} \tag{7}$$

Due to $\Delta n_{\text{eff}} = (\partial n_{\text{eff}}/\partial L)\Delta L$, the remaining terms in (5) omitting the waveguide effect can be transformed into:

$$\Delta\lambda_{Bz} = 2\Delta\left[-\frac{n_{\text{eff}}^3}{2} \cdot \Delta\left(\frac{1}{n_{\text{eff}}^2}\right)\right] + 2n_{\text{eff}} \cdot \varepsilon_{zz} \cdot L \cdot \frac{\partial \Lambda}{\partial L} \tag{8}$$

where $\varepsilon_{zz} = \Delta L/L$ is the longitudinal strain. Due to the existence of formula (6), a simpler expression of $\Delta\lambda_{Bz}$ can be obtained. In fact, in the presence of external stress, the relative dielectric impermeability tensor β_{ij} should be a function of the stress. Taylor expansion of β_{ij} and omission of higher-order terms, using (6) formula, while introducing the elasticity of the material. The coefficient P_{ij} gives:

$$\Delta\left(\frac{1}{n_{\text{eff}}^2}\right) = (P_{11} + P_{12})\varepsilon_{rr} + P_{12}\varepsilon_{zz} \tag{9}$$

where, the axial symmetry of optical fiber $\varepsilon_{rr} = \varepsilon_{\theta\theta}$ is used, and this equation is substituted into Eq. (8) to obtain the relative wavelength drift caused by elastic light effect as follows:

$$\frac{\Delta\lambda_{Bz}}{\lambda_B} = -\frac{n_{\text{eff}}^2}{2}[(P_{11} + P_{12})\varepsilon_{rr} + P_{12}\varepsilon_{zz}] + \varepsilon_{zz} \tag{10}$$

In the formula, the condition that a uniform optical fiber satisfies under uniform stretching is used: $\frac{\partial \Lambda}{\Lambda} \cdot \frac{L}{\partial L} = 1$. Substituting Eq. (4) into the above equation yields:

$$\frac{\Delta\lambda_{Bz}}{\lambda_B} = \left\{ -\frac{n_{\text{eff}}^2}{2}[(P_{11} + P_{12})\nu - P_{12}] - 1 \right\} \cdot |\varepsilon_{zz}| = k \cdot |\varepsilon_{zz}| \tag{11}$$

So the Bragg wavelength change caused by the strain ε_z can be written as:

$$\Delta\lambda_B = \left(K_\varepsilon \cdot \varepsilon + \frac{1}{2}K_{\varepsilon^2} \cdot \varepsilon^2 \right) \cdot \lambda_B \tag{12}$$

For germanium-doped quartz optical fibers, $P_{12} = 0.270, \nu = 0.17, n_{\text{eff}} = 1.456$, and $P_{11} = 0.121$, therefore $P_e \approx 0.22, K_\varepsilon \approx 0.784$. If the 1.3 μm series grating is used, the wavelength drift caused by each micro-strain can be obtained. The typical value of the tension applied to the fiber containing the grating is up to 1% strain. At this time, the error caused by ignoring the second-order sensitivity of the grating does not exceed 0.5%. Therefore, the Bragg wavelength of the fiber grating is better linear with the strain Relationship, the effect of second-order strain sensitivity may not be considered in practical applications [9, 10].

2.2 Basic composition of fiber grating sensor system and sensor network

(1) Sensor detection system

As shown in Fig. 1, the fiber grating sensor detection system consists of two major parts: sensor grating and demodulator. The light emitted by the broadband light source is transmitted in the sensor grating and is to be measured and added to the sensor grating. When the to-be-measured changes, the center wavelength of Bragg's reflected light wave drifts [11]. The error caused by the second-order sensitivity in the grating sensor does not exceed 0.5%. Introduce the demodulator through the coupler to determine the measurement. All kinds of fiber grating sensing and detection systems with more complex functions and better performance are based on this, and improvements are made to each unit [12, 13].

(2) Sensor network

Some measurements are often not a point, but a field with a certain spatial distribution, such as temperature field and stress field. In order to obtain relatively complete information of this type of measured object, it is necessary to use a distributed modulation optical fiber sensing system [14]. The so-called distributed modulation refers to that the external signal field (the measured field) modulates the light waves in the optical fiber in a certain spatial distribution, forms a modulated signal spectrum band in a certain measurement domain, and detects (demodulates) the modulated signal spectrum band. The size and spatial distribution of the external signal field can be measured [15].

One of the main advantages of fiber Bragg grating sensors is that it can easily use wavelength division multiplexing technology to connect multiple Bragg gratings in series in a fiber for distributed measurement. Multiple Bragg gratings connected in series on an optical fiber have different grating constants [16, 17]. The broadband light emitted by the broadband light source passes through all the Bragg gratings through a Y-splitter, and each Bragg grating reflects light of different center wavelengths. The reflected light is coupled into the demodulator through the other port of the Y-splitter. By detecting the wavelength and change of the reflected light through the demodulator, you can know the situation of each Bragg grating being measured [18].

Strictly speaking, the general fiber Bragg grating distributed sensing system should be called a quasi-distributed system, because the fiber Bragg grating distributed sensing system is difficult to realize continuous distribution, but point distribution. However, the length of the Bragg grating can be mm. The life expectancy of practical application is much higher than that of continuous distribution system based on local time technology. The stability of the planet of the continuous distribution system in

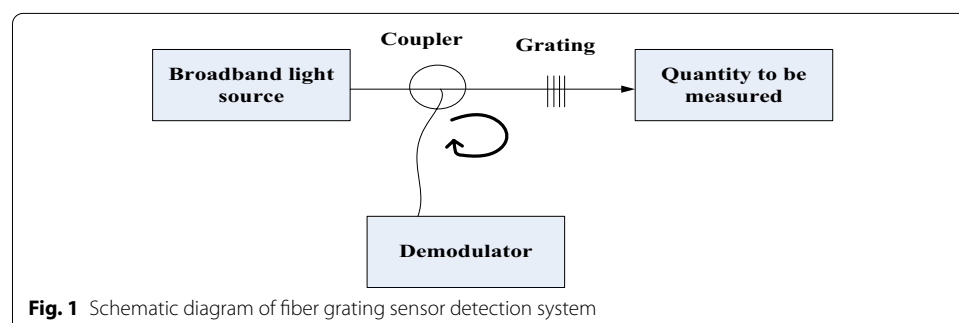


Fig. 1 Schematic diagram of fiber grating sensor detection system

the time field can reach the order of meters only [19, 20]. Therefore, the second-order strain sensitivity has a great influence on the Bragg wavelength and strain of the fiber grating.

2.3 Common demodulation methods of lager grating

(1) Tunable narrow-band laser demodulation method

The biggest difference between the tunable narrowband laser demodulation method and other demodulation methods is that it uses a narrowband tunable laser as the light source of the system. A certain range of scanning voltage is applied to the laser. At this time, the narrow-band laser can periodically output a laser with a continuously changing wavelength. The laser is reflected back by the measured FBG after passing through the coupler, and then detected by the photodetector. When the center wavelength and the center wavelength of the FBG completely coincide, the photodetector can detect the largest electrical signal, and the corresponding center wavelength of the FBG can be obtained [21, 22]. Because the demodulation method uses a laser light source, the method has a high signal-to-noise ratio and resolution, and the structure is simple, but the demodulation method has high cost, slow demodulation speed, and limited tunable range.

(2) Match demodulation method

In the matched demodulation mode, two FBGs need to be used. They are measured FBG1 and matched FBG2. The working principle of matched demodulation is that the light emitted by the broadband light source is reflected by the FBG1 after passing through the coupler, enters the next coupler through the 3 dB coupler 1, and is finally reflected by FBG2. The reflected light undergoes photoelectric conversion to obtain a voltage value. When the center wavelengths of FBG1 and FBG2 completely coincide, the maximum conversion voltage can be achieved [23]. Before compatibility, the correspondence between coupler size and FBG2 wavelength shall be determined. After the control parameters are determined, the specific center wavelength of FBG2, and then obtain the wavelength change adapted to the change of external area, so as to achieve the measurement of the external parameters [24].

Through a detailed comparison of the two, because the tunable narrowband laser demodulation method uses a laser light source, the method has high signal-to-noise ratio and resolution, and has a simple structure. In the matched demodulation mode, two FBGs need to be used, which is costly, and it is also necessary to obtain the specific wavelength of FBG2 by taking the controller level. It can be seen that the tunable narrowband laser demodulation method is more practical.

There are two main types of control equipment:

(1) The use of piezoelectric ceramics as a controller In the use of piezoelectric ceramics as a micro-displacement controller, the reverse piezoelectric effect of piezoelectric ceramics is mainly used. Piezoelectric ceramics will produce strain, deformation and electric field under the action of an electric field. The size is proportional to the direction of deformation is determined by the direction of the applied electric field. Through calibration, the change of FBG2 center wavelength at different voltage values can be obtained. Apply a sawtooth wave voltage to FBG2. When the voltage value after

photoelectric conversion is maximum, the voltage value of the driving power supply can be measured at this time, and the center wavelength value of FBG1 can be obtained [25].

(2) The stepping motor is used as a controller to paste the matched FBG2 on the cantilever arm, and the single-chip microcomputer is used to control the stepper motor. The stepper motor and the free end of the cantilever arm are connected to control the rotation of the stepping motor. The converted electrical signal is collected to realize the compensation of the system wavelength, and the matching of FBG1 is completed. Finally, the central wavelength of FBG1 can be demodulated by collecting the control signal of the single-chip microcomputer.

3 Experiments

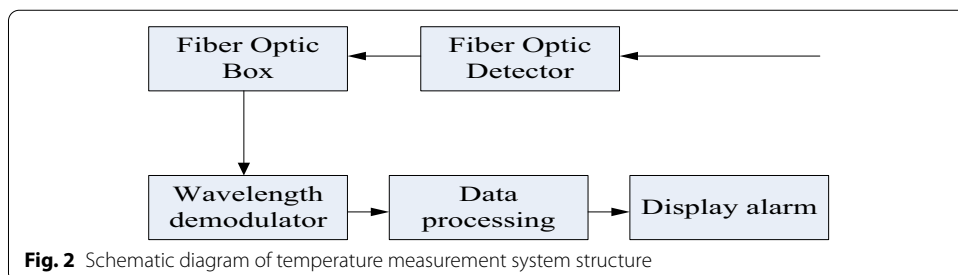
3.1 Design of fiber Bragg grating temperature measurement system

(1) Overall architecture of electrical equipment temperature measurement system based on fiber grating

The entire electrical equipment fiber Bragg grating temperature measurement system is mainly composed of two modules, a fiber grating temperature sensor measurement module and an interface display module. The structure diagram of the temperature measurement system is shown in Fig. 2.

The use of fiber grating in the system has the characteristics of high temperature sensitivity and fast response speed. Real-time temperature distribution and monitoring. When the temperature is abnormally high, the center wavelength will change. We can realize real-time monitoring of cable temperature by real-time monitoring of the center wavelength. We use densely distributed point-type temperature sensors to monitor the temperature of power cables, avoiding the shortcomings of single-point engineering, high cost, and environmental constraints. There is no electricity detection in the cable pit, and the detection data is more accurate; Distributed measurement is adopted, and the system is stable; The optical fiber transmission signal overcomes the electromagnetic interference in the transmission, and the information is accurate and reliable.

The system software module adopts a three-layer architecture of data layer, service layer and client layer. The data layer stores the cable temperature data and cable geographic information data of the data collection part. The service layer server layer mainly includes GIS server, middle layer and Web server, the main function is that when the user sends a request to read data from the client software, the server software will respond accordingly and retrieve the corresponding data from the data layer, and then transmit the data to the client software. The customer can measure the temperature measured by the real-time monitoring sensor, give a temperature



alarm and view the whole wired network image at any time; in the electronic map, the function of querying data and its attributes can also be performed. The entire power monitoring system helps staff to conveniently and timely grasp the complete status of temperature, cable distribution and equipment operation, and provides a timely and reliable basis for scientific management and decision-making. Provide powerful information support for line maintenance, simplify the maintenance preparation and improve efficiency.

(2) System test

The server side of this system uses Microsoft Windows Server 2003 operating system, the Web server uses Microsoft's Internet Information Server (IIS), IIS uses a graphical interface management tool, called the Internet Service Manager, used to monitor, configure and control Internet services IIS allows users to publish information on the public intranet or Internet, so that they can access and modify data information in different locations on the intranet or Internet, further achieving the goal of simultaneous access by multiple users and simultaneous execution of multiple tasks.

After detailed system design and system implementation, it is necessary to conduct preliminary tests on the function and performance of the system to monitor whether the design meets the requirements. According to the project research plan of the electrical equipment temperature online monitoring system, the system is installed and tested with a certain electrical equipment to monitor whether the various functions of the system are operating normally and meet the design requirements.

The intelligent analysis and early warning system is the core part of the online monitoring software and is responsible for the core work of the entire system. The remote diagnosis system mainly includes temperature sensor devices, temperature monitoring various parameter settings, temperature information collection, temperature alarm comprehensive query, analysis and prediction, etc., so the above functions need to be tested. The combination of the intelligent analysis and early warning system and the remote identification system will make the monitoring more accurate.

(1) Temperature data collection and alarm

Test whether the temperature data collection of the sensor is correct, and whether an early warning signal can be issued when the alarm condition is reached. Test method: The temperature measured by the infrared thermometer is compared with that collected by the system, and the temperature range from which the alarm is produced is manufactured.

(2) System analysis and prediction function test

Test whether the analysis capability of the system can work normally, by collecting real-time data, observing the analysis results of the data, and testing by comparing with experience.

(3) Network communication test

Test whether the wireless and other network communication in the system architecture is smooth, carry out remote monitoring on the remote main control end, and whether it can receive real-time temperature data collected by the temperature collector.

(4) Other functional tests

Test other functions in the system, such as system management, users, databases, etc.

Table 1 Fiber Bragg grating temperature measurement results

$t_m/^\circ\text{C}$	29.9273	29.9555	29.8968	29.9439	29.9311
	29.8942	29.8842	29.8742	29.8934	29.8561
	29.9012	29.8274	29.8677	29.9269	29.9328
	29.9113	29.8869	29.8469	29.8671	29.9112

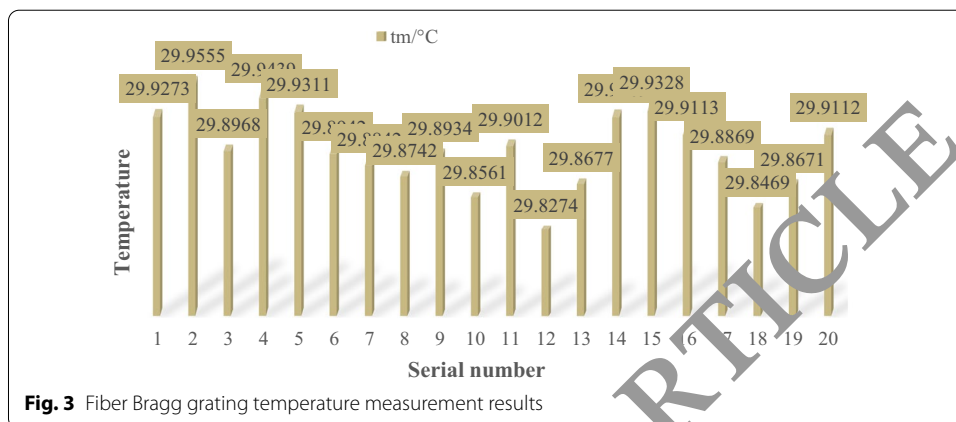


Fig. 3 Fiber Bragg grating temperature measurement results

3.2 Analysis of fiber Bragg grating temperature measurement system

(1) Experimental uncertainty analysis

Measurement uncertainty refers to the uncertainty of the change of the measurement result, which is an estimate of the true value of the measured value within a certain range, a parameter contained in the measurement result, used to characterize the dispersion of the measured value, and is the measurement. An important indicator of result evaluation, the smaller the value, the higher the quality of the measurement result and the greater the use value.

In the actual measurement process, there are many factors that affect the accuracy of the measurement results, so there will be several uncertainty components. Regardless of the nature of these components, they can be evaluated by two types of methods: type A evaluation based on statistical analysis of data And Class B assessments based on experience or scientific estimates made by other relevant information, such as instrument calibration certificates, test reports, technical manuals, etc. Since many uncertainties cannot be evaluated by statistical methods, or although they can be evaluated by statistical methods, the evaluation process is not economically feasible. Therefore, the B-type evaluation method is generally used in practical work.

The system performs 20 continuous temperature measurements under the same measurement conditions. The temperature measurement results at 30 °C after reading the system are shown in Table 1.

As shown in Table 1 and Fig. 3, the sensing distance will not affect the temperature measurement accuracy of the sensor; the single-channel layout of multiple sensors must consider the temperature measurement range and the sensor temperature sensitivity coefficient at the same time; Finally, the source of system uncertainty is

analyzed. The uncertainty is analyzed, and the uncertainty of the calibration result of the fiber grating temperature sensor is 0.0725 °C

(2) Changes in the center wavelength of the fiber grating before and after temperature-sensitive packaging

It is experimentally measured that the center wavelength of the fiber grating will shift toward the direction where the center wavelength becomes smaller after encapsulation. This is mainly caused by the strain characteristics of the fiber grating. When the fiber grating is stressed, it will cause a change in the center wavelength. There are two reasons for this phenomenon: on the one hand, it is due to the elasto-optic effect. The elasto-optic effect reflects the situation where the refractive index changes when the fiber grating is stressed; second, when the grating region of the fiber grating is stressed. The displacement of its microscopic particles is changed, thereby changing the grating period of the fiber grating. These changes will cause the change of the center wavelength of the fiber grating. By analyzing the force, it can be known that the change of the center wavelength of the fiber grating has a linear relationship with the strain. Table 2 shows the drift of the center wavelength of the fiber grating before and after packaging with different substrate materials.

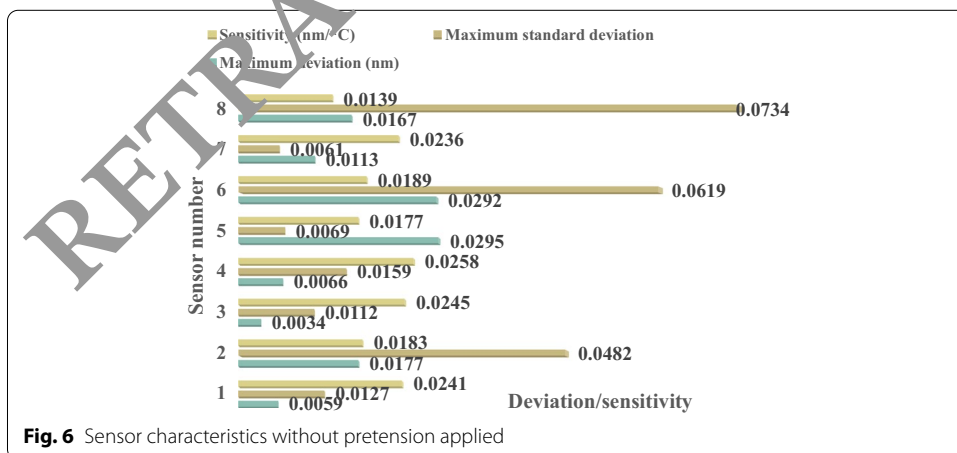
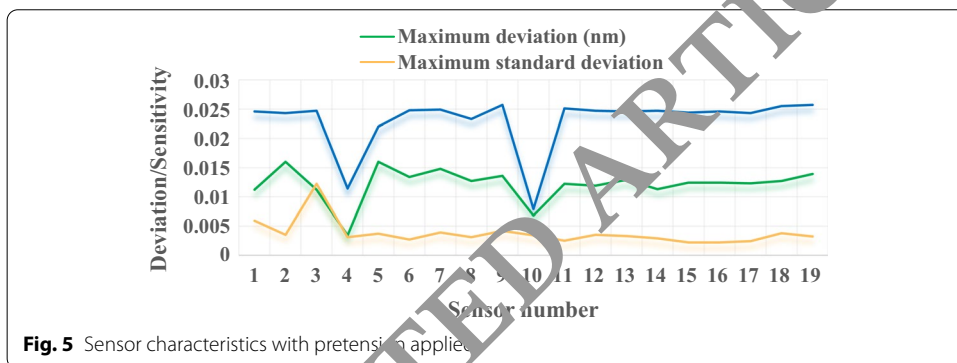
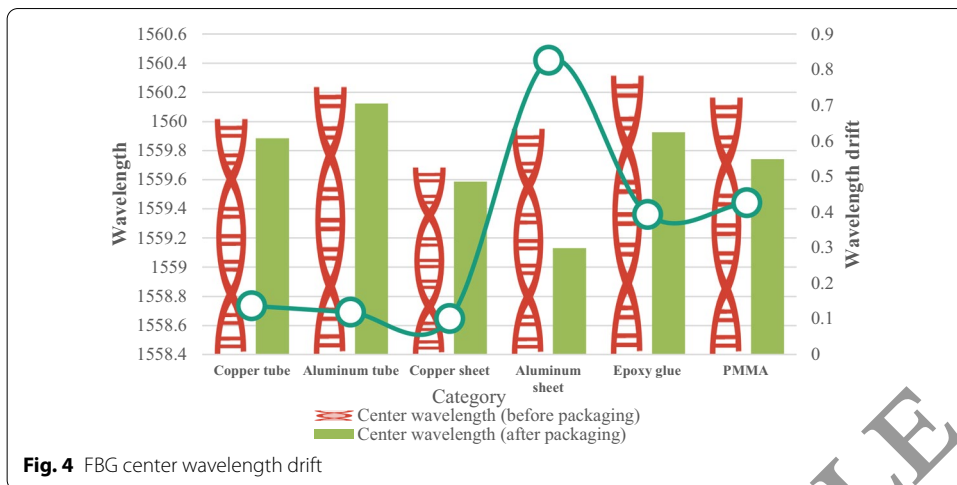
Adjust the initial temperature to 20 °C. After standing for a period of time, record the center wavelength of each fiber grating, and then gradually increase the temperature of the high temperature control box, each increase is 5 °C. Wait until the temperature is stable before recording the center of the fiber grating Wavelength value until the temperature is raised to 80 °C. As shown in Fig. 4, it is the temperature-center wavelength variation curve of different packaged components.

As shown in Fig. 4, compared with bare fiber gratings, the above several packaging methods have improved the temperature sensitivity of fiber gratings, but different types of packaging methods have different temperature sensitivities to fiber gratings. Among them, PMMA and epoxy resin encapsulated fiber gratings have stronger temperature sensitization lines, while metal encapsulated fiber gratings have relatively weaker temperature sensitization, while bare fiber gratings without encapsulation have the weakest temperature sensitivity. This is mainly due to the different thermal expansion coefficients of these materials. The thermal expansion coefficients of PMMA and epoxy resin are much larger than those of metal materials and fiber gratings themselves.

(3) Fiber Bragg grating sensor

Table 2 The drift of the center wavelength of the fiber grating before and after encapsulation with different substrate materials (nm)

Name	Copper tube	Aluminum tube	Copper sheet	Aluminum sheet	Epoxy glue	PMMA
Center wavelength (before packaging)	1560.022	1560.241	1559.688	1559.955	1560.319	1560.168
Center wavelength (after packaging)	1559.885	1560.122	1559.587	1559.129	1559.926	1559.742
Wavelength drift (nm)	0.137	0.119	0.101	0.826	0.393	0.426



As shown in Figs. 5 and 6, the maximum standard deviation of this group of sensors is greater than that of the pre-tensioned packaged sensors. Except for sensors 5 and 7, the maximum standard deviation of the other sensors has reached the order of 10^{-2} .

This indicates that the repeatability of this group of sensors is generally worse than that of sensors with pretension applied.

4 Results and discussion

This study introduced the software part of the calibration system in detail. Firstly, the functions of the built-in software of the fiber Bragg grating temperature measurement system and the distributed fiber temperature measurement system are analyzed, and the design requirements and design schemes of the software system are proposed. Then in the VS2005 development environment, the C++MFC framework is used, combined with SQL Server and MySQL to realize the four module functions of the database: user login, database connection, data reading and operation, and verification report generation. The software can easily process the calibration experimental data of fiber Bragg grating temperature measurement system and distributed fiber temperature measurement system, and improve the experimental efficiency.

In this study, a quasi-distributed experimental scheme was designed with multiple grating temperature sensors as the object, and it was concluded that the sensing distance will not affect the temperature measurement accuracy of the sensor; single-channel deployment of multiple sensors must simultaneously consider the temperature measurement range and the sensor temperature sensitivity coefficient. Finally, the source of system uncertainty is analyzed, and the measurement uncertainty is analyzed. The uncertainty of the calibration result of the fiber Bragg grating temperature sensor is 0.0725 °C.

In this study, by designing a new tube-type temperature-resistant fiber grating sensor with high linearity and sensitivity and small volume, optimizing the structure of the temperature-resistant fiber grating sensor array, a new temperature-resistant fiber grating sensor system based on wavelength demodulation was built, which overcomes based on the shortcomings of the light intensity demodulation temperature-resistant sensing system that is susceptible to the influence of the optical path noise, the experimental analysis of the new temperature-resistant grating sensor center wavelength changes with temperature. The temperature characteristic experiment shows that the system has high accuracy, good stability and response fast time and strong anti-electromagnetic interference ability, it is very suitable for real-time online measurement of temperature in high temperature environment.

Abbreviations

FBG: Fiber Bragg grating; IIS: Internet information server.

Acknowledgements

Not applicable.

Authors' contributions

AP: writing–editing. CL: data analysis. LY: sampling method. All authors read and approved the final manuscript.

Authors' information

Anhua Peng was born in Jian, Jiangxi P. R. China, in 1973. He received the Doctor's degree from China University of Mining and Technology, P.R. China. Now, he works in School of Mechanical Engineering, Jiangsu Ocean University. His research interest fields include measurement technique, signal processing, and multi-criteria decision making.

Chengwen Liu was born in Lianyungang, Jiangsu. P.R. China, in 1968. He received the master's degree from China University of Mining and Technology, P.R. China. Now, he works in School of Mechanical Engineering, Jiangsu Ocean University. His research interests include Sensors and detection technology, quality management.

Le Yang was born in Xuzhou, Jiangsu, P.R. China, in 1977. He received the Ph.D. degree from Wuhan University of Science and Technology, P.R. China. Now, he works in School of Mechanical Engineering, Jiangsu Ocean University. His research interests include lean manufacturing, Sensor technology, knowledge management and engineering.

Funding

Not applicable.

Availability of data and materials

Data sharing not applicable to this article as no datasets were generated or analysed during the current study.

Declarations

Ethical approval and consent to participate

Not applicable.

Consent for publication

Approved.

Competing interests

There is no potential conflict of interest in our paper and all authors have seen the manuscript and approved to submit to your journal. We confirm that the content of the manuscript has not been published or submitted for publication elsewhere.

Author details

¹School of Mechanical Engineering, Jiangsu Ocean University, Lianyungang 222005, Jiangsu, China. Jiangsu Institute of Marine Resources Development, Lianyungang 222005, Jiangsu, China.

Received: 29 June 2021 Accepted: 6 September 2021

Published online: 25 September 2021

References

1. A.K. Singh, S. Berggren, Y. Zhu et al., Simultaneous strain and temperature measurement using a single fiber Bragg grating embedded in a composite laminate. *Smart Mater. Struct.* **26**(11), 115025 (2017)
2. Y. Zhang, Z. Guo, W. Qiao et al., Improved Φ -OTDR system with narrow pulses for quantitative strain measurement based on ultra-weak fiber Bragg grating array. *Microv. Opt. Technol. Lett.* **58**(12), 2892–2894 (2016)
3. X. Gan, Y. Wang, F. Zhang et al., Graphene-controlled fiber Bragg grating and enabled optical bistability. *Opt. Lett.* **41**(3), 603 (2016)
4. Y. Wang, M. Wang, W. Xia et al., Optical fiber Bragg grating pressure sensor based on dual-frequency optoelectronic oscillator. *IEEE Photonics Technol. Lett.* **29**(21), 1864–1867 (2017)
5. R. Ishikawa, H. Lee, A. Lacraz et al., Pressure dependence of fiber Bragg grating inscribed in perfluorinated polymer fiber. *IEEE Photonics Technol. Lett.* **29**(11), 2167–2170 (2017)
6. K. Yang, J. He, C. Liao et al., Femtosecond laser inscription of fiber Bragg grating in twin-core few-mode fiber for directional bend sensing. *J. Lightwave Technol.* **35**(21), 4670–4676 (2017)
7. A. Morana, S. Girard, E. Marin et al., Radiation-hardened fiber Bragg grating based sensors for harsh environments. *IEEE Trans. Nucl. Sci.* **64**(10), 5273 (2017)
8. S. Javdani, M. Fabbian, J.S. Carlton et al., Underwater free-vibration analysis of full-scale marine propeller using a fiber Bragg grating-based sensor system. *IEEE Sens. J.* **16**(4), 946–953 (2016)
9. T. Li, C. Shi, Y. Tan et al., Fiber Bragg grating sensing-based online torque detection on coupled bending and torsional vibration of rotating shaft. *IEEE Sens. J.* **17**(7), 1999–2007 (2017)
10. X. Xu, G. Sun, L. Luo, H. Cao, H. Yu, A.V. Vasilakos, Latency performance modeling and analysis for hyperledger fabric blockchain network. *Inf. Process. Manag.* **58**(1), 102436 (2021)
11. J. P. Domingues, C. Tavares, C. Leitão, et al., Insole optical fiber Bragg grating sensors network for dynamic vertical force monitoring. *J. Biomed. Opt.* **22**(9), 091507 (2017).
12. D. Ganziy, B. Rose, O. Bang, Performance of low-cost few-mode fiber Bragg grating sensor systems: polarization sensitivity and linearity of temperature and strain response. *Appl. Opt.* **55**(23), 6156 (2016)
13. Y. Hu, W. Mo, K. Dong et al., Using maximum spectrum of continuous wavelet transform for demodulation of an overlapped spectrum in a fiber Bragg grating sensor network. *Appl. Opt.* **55**(17), 4670 (2016)
14. J. Kong, X. Ouyang, A. Zhou et al., Pure directional bending measurement with a fiber Bragg grating at the connection joint of eccentric-core and single-mode fibers. *J. Lightwave Technol.* **34**(14), 3288–3292 (2016)
15. C. Kina, K. Turk, E. Atalay et al., Comparison of extreme learning machine and deep learning model in the estimation of the fresh properties of hybrid fiber-reinforced SCC. *Neural Comput Appl.* **33**, 11641–11659 (2021)
16. Y. Jiang, D. Yang, Y. Yuan et al., Strain and high-temperature discrimination using a Type II fiber Bragg grating and a miniature fiber Fabry-Perot interferometer. *Appl. Opt.* **55**(23), 6341 (2016)
17. L. Tong, C. Sheng-Ping, H. Jing, Selective transverse mode operation of an all-fiber laser with a mode-selective fiber Bragg grating pair. *Opt. Lett.* **41**(24), 5692–5695 (2016)
18. Y. Tanaka, H. Miyazawa, Multipoint fiber Bragg grating sensing using two-photon absorption process in silicon avalanche photodiode. *J. Lightwave Technol.* **36**(4), 1032–1038 (2018)
19. F. Zaman, M. Shardlow, S.U. Hassan, N.R. Aljohani, R. Nawaz, HTSS: a novel hybrid text summarisation and simplification architecture. *Inf. Process. Manag.* **57**(6), 102351 (2020)

20. J. Wang, L. Zhao, T. Liu et al., Novel negative pressure wave-based pipeline leak detection system using fiber Bragg grating-based pressure sensors. *J. Lightwave Technol.* **35**(16), 3366–3373 (2017)
21. L. Tianliang, T. Yuegang, H. Xue et al., Diaphragm based fiber Bragg grating acceleration sensor with temperature compensation. *Sensors* **17**(1), 218 (2017)
22. T. Khatti, H. Naderi-Manesh, S.M. Kalantar, Application of ANN and RSM techniques for modeling electrospinning process of polycaprolactone. *Neural Comput. Appl.* **31**, 239–248 (2019)
23. F. Wei, F. Yang, X. Zhang et al., Subkilohertz linewidth reduction of a DFB diode laser using self-injection locking with a fiber Bragg grating Fabry-Perot cavity. *Opt. Express* **24**(15), 17406 (2016)
24. S. Werzinger, S. Bergdolt, R. Engelbrecht et al., Quasi-distributed fiber Bragg grating sensing using stepped incoherent optical frequency domain reflectometry. *J. Lightwave Technol.* **34**(22), 5270–5277 (2016)
25. C.J. Bae, A. Manandhar, P. Kiesel et al., Monitoring the strain evolution of lithium-ion battery electrodes using an optical fiber Bragg grating sensor. *Energy Technol.* **4**(7), 851–855 (2016)

Publisher's Note

Springer Nature remains neutral with regard to jurisdictional claims in published maps and institutional affiliations.

RETRACTED ARTICLE

Submit your manuscript to a SpringerOpen[®] journal and benefit from:

- Convenient online submission
- Rigorous peer review
- Open access: articles freely available online
- High visibility within the field
- Retaining the copyright to your article

Submit your next manuscript at ► [springeropen.com](https://www.springeropen.com)
